Label-free detection of microarrays of biomolecules by oblique-incidence reflectivity difference microscopy

J. P. Landry and X. D. Zhu

Department of Physics, National Science Foundation Center for Biophotonics Science & Technology, University of California at Davis, Davis, California 95616

J. P. Gregg

Department of Pathology, School of Medicine, University of California at Davis, Sacramento, California 95817

Received September 22, 2003

We developed an oblique-incidence reflectivity difference (OI-RD) scanning microscope for label-free imaging of microarrays of biomolecules upon solid substrates. We demonstrate that hybridization reactions in an oligonucleotide microarray fabricated upon a glass slide can be detected by such an OI-RD microscope.

OCIS codes: 180.0180, 170.0170, 310.0310, 240.0240.

Microarrays are micrometer-scale spots of immobilized biological macromolecules arranged in a regular pattern upon a solid substrate.[1] Because of their inherently high spot densities, microarrays enable thousands of biochemical reactions to be investigated in parallel in a high-throughput fashion. Microarrays are usually reacted with fluorophore-labeled probe molecules and are subsequently detected with fluorescence microscopes. For example, on a gene expression profiling microarray[1] each spot consists of a gene fragment that is specific for a particular gene. The gene fragment is either an amplified complementary DNA (cDNA) that is 100–1000 nucleotides long or a synthesized oligonucleotide that is 25–80 nucleotides long. For gene expression profiling, RNA is extracted from a biological sample, such as cells or tissue. It is then converted to fluorophore-labeled cDNA or cRNA and subsequently allowed to react with the gene fragments on the microarray. The fluorescence intensity at each spot is proportional to the number of RNA transcripts of the corresponding gene in the sample.

Fluorescence labeling has been successful for the detection of nucleic acid interactions in microarrays. One reason for this is that the structure and reactivity of nucleic acids are relatively uniform and minimally affected by fluorophore molecules. However, such is not the case for proteins. There are now vigorous efforts to measure protein expression and protein–molecule interactions directly by use of microarrays of protein affinity reagents.[2] Because the structure and reactivity of proteins are much more complex and diverse than those of DNA, the attachment of a fluorophore to a protein may change the way in which the protein binds to other molecules.[3] Furthermore, the efficiency of labeling may vary from protein to protein, making it difficult to measure the relative abundances of a set of unrelated proteins.[4] Label-free detection of reactions in microarrays circumvents these problems. In this Letter we demonstrate that an oblique-incidence optical reflectivity difference (OI-RD) microscope can be used to detect microarrays without labeling.

OI-RD is a particular form of optical ellipsometry that measures optical properties of a thin film upon a substrate.[5,6] At oblique incidence, the reflection for p- and s-polarized light changes disproportionately in response to such a film. Let r_{p0} and r_{s0} be the reflectivities from the bare substrate and r_p and r_s be the reflectivities from the substrate covered with a thin film, and define $\Delta_p = (r_p - r_{p0})/r_{p0}$ and $\Delta_s = (r_s - r_{s0})/r_{s0}$. In the limit that film thickness d is much less than optical wavelength λ, the OI-RD technique permits direct measurements of the real and the imaginary parts of $\Delta_p - \Delta_s$. In terms of the ellipsometric ratio $\rho = r_p/r_s = \tan\psi \exp(i\delta)$,[7] it is easily seen that $\Delta_p - \Delta_s \approx (\rho - \rho_0)/\rho_0$, so $\mathrm{Im}(\Delta_p - \Delta_s) \approx \delta - \delta_0$ and $\mathrm{Re}(\Delta_p - \Delta_s) = 2\csc\psi_0(\psi - \psi_0)$. It has been shown that[5]

$$\Delta_p - \Delta_s \approx -i\left[\frac{4\pi\epsilon_0^{1/2}\epsilon_s \sin^2\theta\cos\theta}{(\epsilon_s - \epsilon_0)(\epsilon_s\cos^2\theta - \epsilon_0\sin^2\theta)}\right] \times \frac{(\epsilon_d - \epsilon_s)(\epsilon_d - \epsilon_0)}{\epsilon_d}\left(\frac{d}{\lambda}\right), \quad (1)$$

where θ is the angle of incidence and ϵ_0, ϵ_d, and ϵ_s are the optical dielectric constants for the ambient, the film, and the substrate, respectively. At a He–Ne laser wavelength of 632 nm, $\epsilon_0 = 1$ (air), $\epsilon_s = 2.31$ (glass slide), and ϵ_d is real for a film of unlabeled DNA. As a result, only $\mathrm{Im}(\Delta_p - \Delta_s)$ is nonzero.

The layout of our OI-RD microscope is shown in Fig. 1. A p-polarized He–Ne laser beam with $\lambda = 632$ nm passes through a photoelastic modulator. The modulator causes the output beam to oscillate at $\Omega = 50$ kHz between p and s polarization. The polarization-modulated beam then passes through a Pockels cell that introduces an adjustable phase ϕ_0 between the s- and p-polarized components. The resultant beam is focused to a 3-μm spot on a microarray-containing surface at incidence angle $\theta = 45°$. After reflection and recollimation the beam passes through an analyzer. The intensity of the transmitted beam $I_R(t)$ is detected with a photodiode and Fourier analyzed with digital lock-in amplifiers. $I_R(t)$ consists of various harmonics of modulation

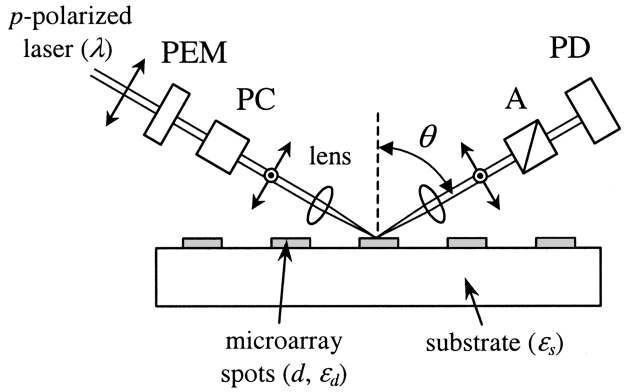

Fig. 1. OI-RD microscope for microarray imaging. The substrate lies upon a pair of translation stages that are movable along the x and y directions: PEM, photoelastic modulator; PC, Pockels cell; A, analyzer; PD, photodiode.

frequency Ω. We detect the first and second harmonics, $I(\Omega)$ and $I(2\Omega)$. Initially the sample is moved to a position where the incident beam reflects off the bare substrate. We adjust the analyzer to zero $I(2\Omega)$ and then adjust phase ϕ_0 (with the Pockels cell) to zero $I(\Omega)$. During the subsequent scan over regions of the surface with features of the microarray, $I(\Omega) \sim \mathrm{Im}(\Delta_p - \Delta_s)$ and $I(2\Omega) \sim \mathrm{Re}(\Delta_p - \Delta_s)$. The proportionality constants are measured separately, so $\Delta_p - \Delta_s$ is determined absolutely.[8] In the present study we record only $\mathrm{Im}(\Delta_p - \Delta_s)$ images by moving the sample underneath the fixed optics.

The oligonucleotide microarrays were fabricated by use of a pin-and-ring contact-printing robot (Genetic Microsystems GMS 417). We printed 60-base oligonucleotides (Sigma-Genosys) dissolved in ultrapure nuclease-free water on poly-L-lysine coated glass slides (CEL Associates). The printing pin's diameter was 125 μm, and the volume of the deposited solution was 1.5 nL. At neutral pH, negatively charged oligonucleotides bind electrostatically to positively charged amino groups on the poly-L-lysine coated slide.[9] After printing, we irradiated the microarrays with UV light ($\lambda = 254$ nm) at a dosage of 60 mJ/cm^2 to induce covalent bonds.[10] We washed off excess oligonucleotides by immersing the printed glass slide in a sodium borate buffer (pH 8.5) for 4 min. The remaining amino groups on the glass slide were blocked with succinic anhydride in borate-buffered 1-methyl-2-pyrolidinone for 1 h.[10] Hybridization reactions took place in a mixture of 3× saline sodium citrate, 0.2% sodium dodecyl sulfate, and 2-μM 60-base oligonucleotide probe at 25 °C for 2 h. The probe concentration was high enough to ensure complete hybridization between the complementary probe and the printed oligonucleotides.

Figure 2(a) shows an $\mathrm{Im}(\Delta_p - \Delta_s)$ image of the microarray before hybridization. Each column was printed with unlabeled oligonucleotides of unique sequence: 5′-TCACAAACCC GTCCTACTCT ACTAGCTGCA GTAGCCCCAC TGGTTCCCGT TTCCGATGTT-3′ for column 1, 5′-CCTTGTACCG CTGAGTTCAC ACCGACACAC CTCACCACAC TTACACCGTC CACAAAGAGA-3′ for column 2, and 5′-TTTCCATGCG GACCTACCAC CGTAGTACCT CGCAATGCCA GTGCAACAAG TACACCTGGA-3′ for column 3. Before imaging, the printed microarray was washed to remove excess oligonucleotides on top of a saturated monolayer. In our experiment the printing concentration was in excess of 42 μM to ensure the saturation condition (see Fig. 3). The top spot in column 3 (Fig. 2) was left blank for alignment control. The eight spots in this image have roughly equal values of $\mathrm{Im}(\Delta_p - \Delta_s)$. Figure 2(b) shows the $\mathrm{Im}(\Delta_p - \Delta_s)$ image after the microarray has been hybridized with a solution of unlabeled oligonucleotides complementary to column 1 and Cy5-labeled oligonucleotides complementary to column 3. For quality control, column 2 was not reacted. Figure 2(c) shows a Cy5-fluorescence image of the microarray (acquired with Genetic Microsystems GMS 418 fluorescence scanner) after hybridization, revealing the two hybridized spots in column 3. The image confirms that the solution-phase oligonucleotides bound only to the complementary oligonucleotides that were printed on the glass slide. Figure 2(d) shows the differential

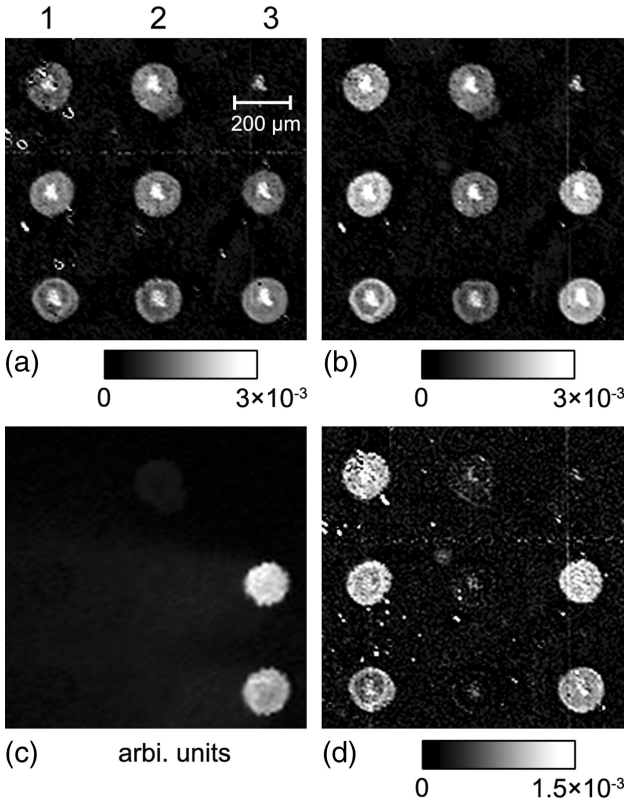

Fig. 2. OI-RD and fluorescence scans of a microarray of 60-base oligonucleotides before and after hybridization. Columns 1–3 are printed with different oligonucleotides. The top position in column 3 was left blank for alignment. (a) $\mathrm{Im}(\Delta_p - \Delta_s)$ image of the printed microarray before hybridization; (b) $\mathrm{Im}(\Delta_p - \Delta_s)$ image of the microarray after hybridization with an unlabeled oligonucleotide complementary to column 1 and a Cy5-labeled oligonucleotide complementary to column 3; (c) Cy5 fluorescence image after hybridization; (d) differential $\mathrm{Im}(\Delta_p - \Delta_s)$ image obtained by subtraction of (a) from (b), revealing hybridized spots in both column 1 (label free) and column 3 (Cy5 labeled).

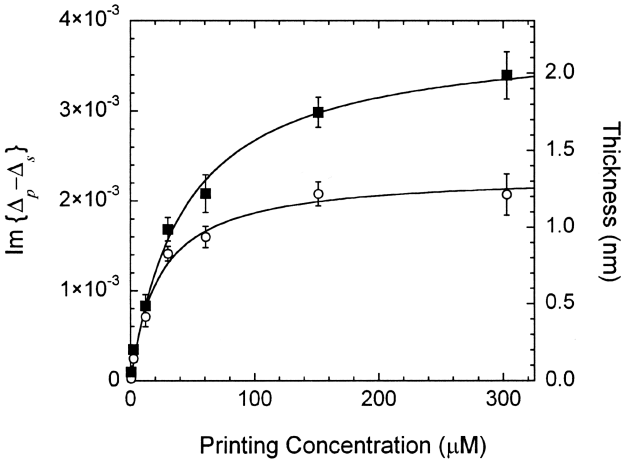

Fig. 3. $\mathrm{Im}(\Delta_p - \Delta_s)$ averaged over the area of a printed spot versus printing concentration: open circles, before hybridization; filled squares, after hybridization.

$\mathrm{Im}(\Delta_p - \Delta_s)$ image obtained by subtraction of Fig. 2(a) from Fig. 2(b). In contrast to the fluorescence image, the differential $\mathrm{Im}(\Delta_p - \Delta_s)$ image reveals hybridization in both column 1 (label free) and column 3 (Cy5 labeled) with almost equal contrast. The variations in the OI-RD images are caused by a combination of the printing process and mechanical error in our current scan system and can be significantly improved.

We now present a quantitative analysis of the optical signal in which we use Eq. (1) to determine the thickness of oligonucleotides in the microarray before and after hybridization. In Fig. 3 we plot the spatially averaged $\mathrm{Im}(\Delta_p - \Delta_s)$ over the printed spot area (after the excess oligonucleotides are removed) relative to printing concentration. Each point is the mean of four replicate spots printed at separate locations on the microarray, and the error bars are the standard deviations. $\mathrm{Im}(\Delta_p - \Delta_s)$ levels off to 2.0×10^{-3} for all spots printed with concentrations in excess of 40–50 μM, indicating that a stably bound monolayer of oligonucleotides forms upon the poly-L-lysine coated glass slide with a density near saturation. The error bars in Fig. 3 show the variation in $\mathrm{Im}(\Delta_p - \Delta_s)$ among spots that were printed at the same concentration. The actual detection limit of our current microscope is at least 1 order of magnitude smaller than the smallest error bar shown. Near the saturation density, the dielectric constant of the oligonucleotide monolayer[11] is expected to be $\epsilon_d = 2.14$. Using Eq. (1) and $\epsilon_d = 2.14$, we found that the thickness of the unlabeled oligonucleotide monolayer before hybridization is 1.2 nm, very close to the diameter of a single-stranded oligonucleotide. This means that the 60-base oligonucleotides lie more or less flat upon the substrate.[9] After hybridization [Fig. 2(d)], assuming that the molecular density remains constant, the increase in $\mathrm{Im}(\Delta_p - \Delta_s)$ by 1.0×10^{-3} corresponds to a change of 0.6 nm in thickness. Inasmuch as the printed film inevitably contains sterically inaccessible oligonucleotides, because of entanglement, for example, a change in film thickness of less than 1 nm after nearly complete hybridization is expected.

Other label-free methods, most notably surface plasmon resonance microscopy[12] and mass spectrometry,[13] exist for microarray detection. Mass spectrometry requires that microarrays be fabricated upon a special matrix medium for laser-induced desorption and ionization. The sensitivity of surface plasmon resonance microscopy derives from the sharp resonance of the plasmon surface polariton and thus requires microarrays to be fabricated on functionalized gold films. In comparison, the OI-RD microscope requires only optically flat substrates, which give flexibility in the choice of immobilization chemistry used in microarray fabrication. For example, we have used chemically modified glass substrates that are in widespread use for fluorescence detection of microarrays. The scanning OI-RD microscope can also be configured into a nonscanning microscope by use of two-dimensional detectors such as CCDs. Furthermore, similarly to surface plasmon resonance microscopes, the OI-RD microscope is an *in situ* detection method that permits high-throughput parallel assays of biochemical kinetics and noninvasive imaging of microarrays at intermediate processing steps.

In conclusion, we have demonstrated that an oblique-incidence reflectivity difference microscope can quantitatively detect a microarray of biological macromolecules without labeling. Such a microscope is particularly useful in investigations of biochemical processes in microarrays that may be adversely influenced by labeling agents.

This research was supported by the National Science Foundation under grant DMR-9818483 and by the National Science Foundation Center for Biophotonics Science & Technology under grant PHY0120999. X. D. Zhu's e-mail address is xdzhu@ucdphy.ucdavis.edu.

References

1. M. Schena, *Microarray Analysis* (Wiley, Hoboken, N.J., 2003), pp. 1–23.
2. S. P. Gygi, Y. Rochon, B. R. Franza, and R. Aebersold, Mol. Cell Biol. **19,** 1720 (1999).
3. G. MacBeath, Nature Genet. **32,** 526 (2002).
4. P. Mitchell, Nature Biotech. **20,** 225 (2002).
5. A. Wong and X. D. Zhu, Appl. Phys. A **63,** 1 (1996).
6. X. D. Zhu, H. B. Lu, G. Z. Yang, Z. Y. Li, B. Y. Gu, and D. Z. Zhang, Phys. Rev. B **57,** 2514 (1998).
7. R. M. A. Azzam and N. M. Bashara, *Ellipsometry and Polarized Light* (Elsevier, New York, 1987), p. 305.
8. J. Gray, P. Thomas, and X. D. Zhu, Rev. Sci. Instrum. **72,** 3714 (2001).
9. S. V. Lemeshko, T. Powdrill, Y. Y. Belosludtsev, and M. Hogan, Nucl. Acids Res. **29,** 3051 (2001).
10. M. D. Eisen and P. O. Brown, Methods Enzymol. **303,** 179 (1999).
11. D. E. Gray, S. C. Case-Green, T. S. Fell, P. J. Dobson, and E. M. Southern, Langmuir **13,** 2833 (1997).
12. J. M. Brockman, B. P. Nelson, and R. M. Corn, Annu. Rev. Phys. Chem. **51,** 41 (2000).
13. E. Scrivener, R. Barry, A. Platt, R. Calvert, G. Masih, P. Hextall, M. Soloviev, and J. Terrett, Proteomics **3,** 122 (2003).